Transition-metal Complexes of Cyclohexane-1,2-dione Bis(thiosemicarbazone) (H_2L). Crystal Structures of $[ZnL(OH_2)]$·dmf (dmf = Dimethylformamide) and $[Zn(H_2L)Cl]Cl·2H_2O$ †

Maria C. Rodríguez-Argüelles,[a] Luigi Pietro Battaglia,[b] Marisa Belicchi Ferrari,[b] Giovanna Gasparri Fava,[b] Corrado Pelizzi[b] and Giorgio Pelosi[b]

[a] *Departamento de Quimica Pura e Aplicada, Universidade de Vigo, 36200 Vigo, Spain*

[b] *Dipartimento di Chimica Generale ed Inorganica, Chimica Analitica, Chimica Fisica, Centro di Studio per la Strutturistica Diffrattometrica del C.N.R., Viale delle Scienze, 43100 Parma, Italy*

The reaction of chlorides and acetates of Fe^{II}, Ni^{II}, Cu^{II} and Zn^{II} with the polydentate ligand cyclohexane-1,2-dione bis(thiosemicarbazone) (H_2L) led to the formation of some novel complexes which have been characterized by spectroscopic methods (NMR, IR). The crystal structures of the two compounds $[ZnL(OH_2)]$·dmf (dmf = dimethylformamide) **1** and $[Zn(H_2L)Cl]Cl·2H_2O$ **2** have been determined. In both complexes the co-ordination geometry about zinc is distorted square-planar pyramidal. The axial sites are occupied by a water molecule in **1** or by a chlorine atom in **2**. The ligand is dideprotonated in **1** and neutral in **2**, so that in **1** a higher π-delocalization is observed.

We have previously examined the ligand behaviour of aliphatic and heterocyclic monothiosemicarbazones in several transition metal complexes[1-3] with the aim of gaining more information about their co-ordination and related biological and pharmacological properties.

As an extension of this we have now considered the chelating properties of the polydentate ligand cyclohexane-1,2-dione bis(thiosemicarbazone) (H_2L) in order to verify the effect of two $NNHC(S)NH_2$ systems on co-ordination to metal atoms.

This paper reports the syntheses and the spectroscopic (NMR, IR) characterization of complexes obtained by reaction of H_2L with chlorides and acetates of Fe^{II}, Ni^{II}, Cu^{II} and Zn^{II}. In particular, following our investigations of zinc complexes as models for zinc–sulfur centres in metalloproteins[3,4] we also describe the crystal structures of two new zinc compounds: aqua[cyclohexane-1,2-dionebis(thiosemicarbazonato)]zinc(II)–dimethylformamide (dmf) (1/1), $[ZnL(OH_2)]$·dmf **1** and chloro[cyclohexane-1,2-dione bis(thiosemicarbazone)]zinc(II) chloride dihydrate, $[Zn(H_2L)Cl]Cl·2H_2O$ **2**.

Experimental

Measurements.—Elemental analyses were performed on a Carlo Erba Instrument CHNS-O EA 1108 automatic analyser and melting points determined in a Büchi apparatus. Infrared spectra for KBr discs were recorded on a Nicolet 5PCFT-IR spectrophotometer and ^1H and ^{13}C NMR spectra at room temperature on a Bruker AMX300 instrument and referred to $SiMe_4$ using the $(CD_3)_2SO$ solvent signals (^1H, δ 2.48; ^{13}C, δ 39.51).

Materials.—All reactants and solvents were of reagent grade. Thiosemicarbazide was obtained from Merck and cyclohexane-1,2-dione from Aldrich.

Preparations.—*Cyclohexane-1,2-dione bis(thiosemicarbazone).* The bis(thiosemicarbazone) H_2L was obtained by reacting cyclohexane-1,2-dione and thiosemicarbazide (1:2 molar ratio) in a methanol–water solution, following the procedure previously described for other bis(thiosemicarbazones).[4]

$Fe(H_2L)Cl_2·0.5EtOH$. An ethanol suspension (50 cm^3) of iron chloride (0.21 g, 1.7 mmol) and H_2L (0.43 g, 1.7 mmol) was refluxed for 4 h under a nitrogen atmosphere. The black solid formed was filtered off and dried under vacuum (Found: C, 26.4; H, 4.0; N, 20.2; S, 16.6. Calc. for $C_9H_{17}Cl_2FeN_6O_{0.5}S_2$: C, 26.5; H, 4.2; N, 20.6; S, 15.7%); m.p. 217 °C.

An ethanol suspension (50 cm^3) of iron acetate (0.09 g, 0.5 mmol) and H_2L (0.13 g, 0.15 mmol) was refluxed for 3 h under a nitrogen atmosphere. After slow evaporation of the solvent, a mixture of unidentified black solids was obtained.

$Ni(H_2L)Cl_2$. An ethanol solution (20 cm^3) of nickel chloride (0.10 g, 0.4 mmol) was added to a hot ethanol suspension (30 cm^3) of H_2L (0.11 g, 0.4 mmol). The mixture was refluxed for 5 h, and after cooling a brown solid was isolated and dried under vacuum (Found: C, 24.5; H, 3.2; N, 21.5; S, 17.1. Calc. for $C_8H_{14}Cl_2N_6NiS_2$: C, 24.8; H, 3.6; N, 21.7; S, 16.5%); m.p. 248 °C.

NiL. A solution of nickel acetate (0.11 g, 0.5 mmol) in ethanol (25 cm^3) was added, dropwise, to an ethanol suspension (30 cm^3) of H_2L (0.12 g, 0.5 mmol). The mixture was heated (at 50 °C) and stirred for 6 h. After cooling a red-brown solid was obtained, filtered off and vacuum dried (Found: C, 30.8; H, 3.8; N, 25.3; S, 20.6. Calc. for $C_8H_{12}N_6NiS_2$: C, 30.5; H, 3.8; N, 26.6; S, 20.3%); m.p. > 300 °C.

$Cu(H_2L)Cl_2$. A hot ethanol suspension (30 cm^3) of H_2L (0.26 g, 1 mmol) was added to an ethanol solution (20 cm^3) of copper chloride (0.17 g, 1 mmol). The mixture was refluxed for 5 h and after cooling a dark green solid was isolated (Found: C, 24.7; H, 3.5; N, 21.2; S, 17.2. Calc. for $C_8H_{14}Cl_2CuN_6S_2$: C, 24.5; H, 3.6; N, 21.4; S, 16.3%); m.p. 210 °C.

CuL·0.5EtOH. An ethanol solution (20 cm^3) of copper acetate (0.10 g, 0.8 mmol) was added to a suspension of H_2L (0.21 g, 0.8 mmol) in ethanol (20 cm^3) and refluxed for 6 h, and the green-brown solid formed filtered off (Found: C, 30.9; H,

† *Supplementary data available:* see Instructions for Authors, *J. Chem. Soc., Dalton Trans.*, 1995, Issue 1, pp. xxv–xxx.

Table 1 Crystal data and refinement details

Compound	**1**	**2**
Formula	$C_{11}H_{21}N_7O_2S_2Zn$	$C_8H_{18}Cl_2N_6O_2S_2Zn$
M	412.8	430.7
Space group	$C2/c$	$P2_1/n$
a/Å	21.180(5)	15.074(2)
b/Å	14.454(3)	13.574(2)
c/Å	14.754(3)	7.803(1)
β/°	129.13(6)	92.70(2)
U/Å^3	3504(3)	1594.8(4)
Z	8	4
D_c/g cm^{-3}	1.56	1.79
$F(000)$	1712	880
Crystal size/mm	0.44 × 0.23 × 0.18	0.49 × 0.23 × 0.16
μ/cm^{-1}	43.5	78.0
Scan speed/°min^{-1}	2.5–12	3–12
θ range/°	3–70	3–70
No. of reflections measured	3620	3567
No. of reflections used in the refinement [$I > 3\sigma(I)$]	2416	2797
No. of refined parameters	227	262
$R = \Sigma\|\Delta F\|/\Sigma\|F_o\|$	0.0607	0.0653
$R' = [\Sigma w(\Delta F^2)/\Sigma w F_o^2]^{\frac{1}{2}}$	0.0673	—
k,g in $w = k/[\sigma^2(F_o) + gF_o^2]$	3.0, 6.43 × 10^{-4}	*
Maximum, minimum, height in final ΔF map/e Å^{-3}	0.51, −0.22	0.37, −0.74

* Unit weights.

4.0; N, 24.4; S, 19.3. Calc. for $C_9H_{15}CuN_6O_{0.5}S_2$: C, 31.3; H, 4.4; N, 24.4; S, 18.6%); m.p. 228 °C.

$Zn(H_2L)Cl_2$·EtOH. An ethanol solution (15 cm^3) of zinc chloride (0.15 g, 1 mmol) was added slowly to a hot ethanol suspension (50 cm^3) of H_2L (0.29 g, 1 mmol). The yellow solution was refluxed for 6 h and the solid formed at room temperature was filtered off and vacuum dried (Found: C, 26.8; H, 4.8; N, 18.2; S, 14.4. Calc. for $C_{10}H_{20}Cl_2N_6OS_2Zn$: C, 27.3; H, 4.6; N, 19.0; S, 14.5%); m.p. 238 °C.

When $Zn(H_2L)Cl_2$·EtOH was dissolved in dimethylformamide yellow crystals were isolated which on the basis of the analytical data and the X-ray diffraction analysis are consistent with $[ZnL(OH_2)]$·dmf **1**.

The compound $Zn(H_2L)Cl_2$·EtOH was dissolved in methanol and after several days yellow crystals of $[Zn(H_2L)Cl]Cl·2H_2O$ **2** were isolated (Found: C, 22.3; H, 4.2; N, 19.5; S, 14.8. Calc. for $C_8H_{18}Cl_2N_6O_2S_2Zn$: C, 23.3; H, 3.9; N, 20.3; S, 15.5%).

ZnL·EtOH. An ethanol solution of zinc acetate (0.11 g, 0.5 mmol) was added to an ethanol suspension (25 cm^3) of H_2L (0.13 g, 0.5 mmol). The resultant solution was refluxed for 4 h and a yellow-brown powdery precipitate was obtained on cooling. The solid was filtered off and vacuum dried (Found: C, 33.5; H, 4.7; N, 22.4; S, 17.8. Calc. for $C_{10}H_{18}N_6OS_2Zn$: C, 32.7; H, 4.9; N, 22.8; S, 17.4%); m.p. 289 °C.

From the solution of ZnL·EtOH in dimethylformamide, yellow crystals of $[ZnL(OH_2)]$·dmf **1** were obtained after several days (Found: C, 32.7; H, 5.5; N, 23.2; S, 14,8. Calc. for $C_{11}H_{21}N_7O_2S_2Zn$: C, 32.0; H, 5.1; N, 23.7; S, 15.5%).

Crystal Structure Analyses.—Crystals of both compounds were mounted in a random orientation on a Siemens AED single crystal automated diffractometer: the resulting crystal data and details concerning data collection and refinements are given in Table 1. After the usual data reduction an empirical correction for absorption was applied following Walker and Stuart's method.[5] The structures were solved by the heavy-atom technique starting from a three-dimensional Patterson analysis using the SHELXS-86[6] program for compound **1** and by direct methods using the SIR92[7] program for **2**. For both compounds successive Fourier syntheses gave coordinates of all non-hydrogen atoms which were refined by full matrix least-squares with anisotropic thermal parameters using the SHELX 76[8] system of computer programs. Hydrogen atoms were located from a ΔF map and introduced in the last refinement cycles for **1**, while for **2** these were partly located and partly calculated at their geometrical positions and mantained as fixed contributors in the last calculation. The atomic scattering factors were taken from ref. 9. The final atomic coordinates are given in Tables 2 and 3 for **1** and **2** respectively.

All calculations were performed on a GOULD 6040 Powernode and ENCORE 91 computers at the Centro di Studio per la Strutturistica Diffrattometrica del C.N.R. (Parma) using the PARST[10] program for the geometrical description of the structures and ORTEP[11] and PLUTO[12] for the structure drawings.

Table 2 Atomic coordinates (× 10^4) for **1** with estimated standard deviations (e.s.d.s) in parentheses

Atom	X/a	Y/b	Z/c
Zn	3919.2(4)	3211.9(5)	3945.4(6)
S(1)	3006.6(9)	4398.1(1.0)	3516.3(1.4)
S(2)	3267.0(9)	1833.5(1.0)	2969.2(1.6)
O(1)	4437(3)	3636(3)	3219(4)
N(1)	3517(4)	5989(4)	4586(6)
N(2)	4493(3)	4889(3)	5569(4)
N(3)	4659(3)	3971(3)	5526(4)
N(4)	4803(3)	2257(3)	5215(4)
N(5)	4767(3)	1331(3)	4980(4)
N(6)	3979(4)	217(4)	3614(5)
C(1)	3747(3)	5113(4)	4652(5)
C(2)	5311(3)	3584(4)	6410(5)
C(3)	5950(4)	4047(4)	7543(5)
C(4)	6638(5)	3419(5)	8482(7)
C(5)	6375(6)	2464(5)	8432(7)
C(6)	6015(5)	2004(5)	7258(6)
C(7)	5373(3)	2575(4)	6245(5)
C(8)	4076(4)	1106(4)	3961(5)
O(f)	9118(6)	2447(8)	6325(9)
C(1f)	9109(14)	3378(19)	6285(21)
C(2f)	7877(10)	3530(13)	4501(16)
C(3f)	8666(9)	4877(11)	5848(14)
N(f)	8536(5)	3897(6)	5491(7)

Table 3 Atomic coordinates (× 10^4) for **2** with e.s.d.s in parentheses

Atom	X/a	Y/b	Z/c
Zn	6 558.5(6)	4 015.8(7)	7 806.7(13)
Cl(1)	7 168(1)	4 495(1)	5 302(3)
Cl(2)	9 959(1)	3 163(2)	11 615(4)
S(1)	6 931(1)	2 348(1)	8 390(3)
S(2)	5 083(1)	4 338(1)	7 314(3)
N(1)	8 450(4)	1 833(4)	9 703(10)
N(2)	8 185(4)	3 465(4)	9 835(9)
N(3)	7 640(4)	4 240(4)	9 595(8)
N(4)	6 466(4)	5 453(4)	9 030(8)
N(5)	5 763(4)	6 005(4)	8 659(9)
N(6)	4 433(4)	6 132(5)	7 519(11)
C(1)	7 904(4)	2 565(5)	9 334(10)
C(2)	7 790(4)	5 079(5)	10 281(10)
C(3)	8 559(5)	5 353(6)	11 356(12)
C(4)	8 383(5)	6 213(6)	12 545(12)
C(5)	8 001(5)	7 064(6)	11 572(12)
C(6)	7 124(5)	6 816(5)	10 736(10)
C(7)	7 094(4)	5 804(5)	9 950(10)
C(8)	5 098(4)	5 548(5)	7 849(10)
O(1)	5 284(4)	7 896(4)	9 384(10)
O(2)	4 177(5)	272(6)	1 872(13)

Additional material available from the Cambridge Crystallographic Data Centre comprises H-atom coordinates, thermal parameters and remaining bond lengths and angles.

Results and Discussion

Crystal and Molecular Structures.—The structure of complex **1** is composed of discrete neutral molecular units of $[ZnL(OH_2)]$ and dimethylformamide as solvate, while the structure of **2** consists of $[Zn(H_2L)Cl]^+$ cations, Cl^- anions and water molecules of crystallization.

Figs. 1 and 2 show the co-ordination environment of the zinc atoms for the complexes **1** and **2** respectively. Both compounds contain five-co-ordinated metal atoms in a distorted square-planar pyramidal arrangement in which the N,N′,S,S′ donor atoms of the tetradentate ligand define the base. The axial sites are occupied by a water molecule in complex **1** or by a chlorine atom in **2**. The zinc atoms are displaced out of the basal planes by 0.488(1) and 0.548(1) Å for **1** and **2** respectively towards the atoms at the apex of the pyramid. The angles formed by the Zn–O and Zn–Cl bonds with the normal to the basal planes are 4.6 and 6.8° respectively.

The Zn–O apical bond in **1** is in agreement with other Zn–O distances reported in the literature and the corresponding Zn–Cl(1) distance in **2** falls in the range of the highest values for non-bridging Zn–Cl bonds,[3] which may be related to the fact that Cl(1) accepts three hydrogen bonds (Table 7).

In **1** the two Zn–S and the two Zn–N distances are similar, as are the angles in the basal plane involving these atoms: Zn–S 2.333(2), 2.352(2) and Zn–N 2.120(4), 2.118(4) Å. Similar trends were found in the structure of aqua[3-ethoxy-2-oxobutyraldehyde bis(thiosemicarbazonato)]zinc(II), $[ZnL'(OH_2)]$ **3**,[13] as seen in Table 4.

Complex **2** exhibits more asymmetry both in the co-ordination distances [Zn–S 2.371(2), 2.282(2) Å, Zn–N 2.117(6), 2.179(6) Å] and in the two thiosemicarbazonic chains: the C(1)–N(1), C(1)–N(2) and N(2)–N(3) distances are longer than the corresponding C(8)–N(6), C(8)–N(5) and N(5)–N(4) distances (Table 5). This may be related to the different electronic structures of the ligand and probably to the strong N(2)–H · · · Cl(2) hydrogen bond [2.984(6) Å] which is shorter than the sum of the van der Waals radii, 3.30 Å.[14] Moreover the S(2)N(6)C(8)N(5)N(4) fragment is perfectly planar, while S(1)N(1)C(1)N(2)N(3) deviates considerably from planarity [the largest deviation from the best plane being 0.024(7) Å for N(2)]. In **1** a higher π-delocalization is observed [C–S = 1.737(5), 1.738(5) Å] which affects the whole dideprotonated thiosemicarbazonic system, as was also observed in the similar complex $[ZnL'(OH_2)]$[13] (Table 5). In **2**, probably owing to the absence of deprotonation, the C–S bonds retain a partial double-bond character [1.637(7), 1.694(7) Å]. The differences within the ligand moieties for both complexes are also highlighted by comparison of the torsion angles (Table 6).

In both complexes the ligand is not planar and gives rise to three five-membered chelate rings which show an envelope conformation. The puckering parameters[15] are: $q_2 = 0.285(5)$, $\varphi_2 = -176(1)$ in **1** and $q_2 = 0.259(6)$ Å, $\varphi_2 = -179(1)°$ in **2** for the ZnN(3)N(2)C(1)S(1) ring; $q_2 = 0.140(5)$, $\varphi_2 = 1(3)$ in **1** and $q_2 = 0.230(5)$ Å, $\varphi_2 = -176(2)°$ in **2** for the ZnN(4)N(5)C(8)S(2) ring; and $q_2 = 0.103(7)$, $\varphi_2 = -157(4)$ in **1** and $q_2 = 0.131(7)$ Å, $\varphi_2 = -180(3)°$ in **2** for the ZnN(3)C(2)C(7)N(4) ring. The dihedral angles between the

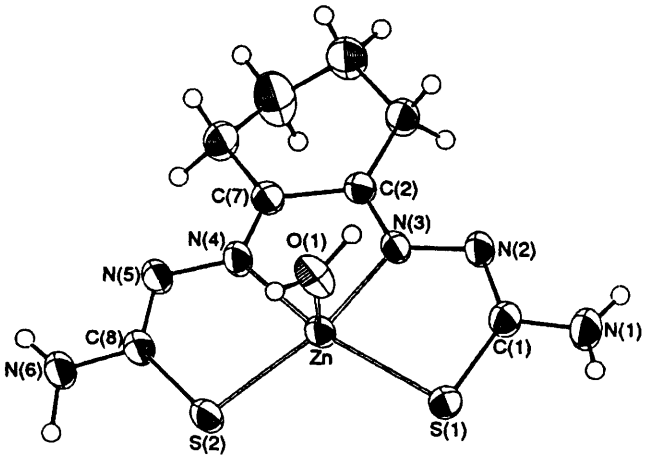

Fig. 1 Perspective view of $[ZnL(OH_2)]$ (thermal ellipsoids at the 50% probability level)

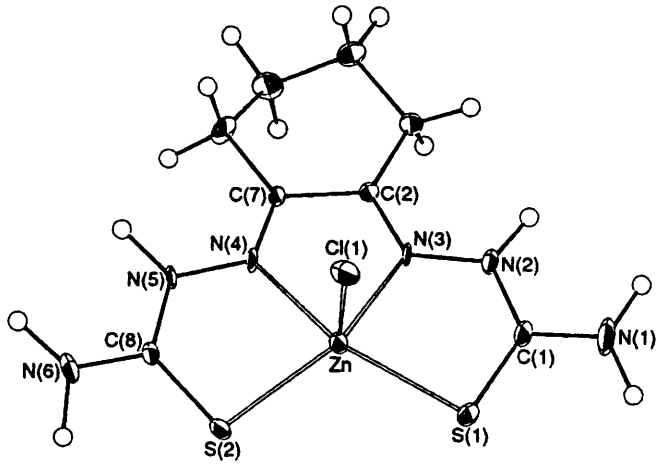

Fig. 2 Perspective view of the cation $[Zn(H_2L)Cl]^+$ (thermal ellipsoids at the 50% probability level)

Table 4 Co-ordination distances (Å) and angles (°) around the metal atom for $[ZnL(OH_2)]$·dmf **1** (X = O), $[Zn(H_2L)Cl]Cl·2H_2O$ **2** (X = Cl) and $[ZnL'(OH_2)]$ **3** (X = O)[13]

Complex	Zn–S	Zn–N	Zn–X	Complex	S–Zn–S	N–Zn–N	S–Zn–N	X–Zn–S	X–Zn–N
1	2.352(2)	2.118(4)	2.052(8)	**1**	112.99(6)	74.8(2)	80.2(1)	105.1(2)	101.0(2)
	2.333(2)	2.120(4)					80.7(1)	103.6(2)	98.8(2)
2	2.371(2)	2.117(6)	2.292(2)				146.1(1)		
	2.282(2)	2.179(6)					149.4(1)		
3	2.357(2)	2.148(4)	2.091(3)	**2**	115.82(7)	69.3(2)	80.9(2)	109.48(7)	101.2(2)
	2.361(2)	2.126(4)					79.6(2)	103.21(8)	99.0(2)
							142.9(2)		
							142.2(2)		
				3	118.11(6)	74.3(1)	80.7(1)	104.6(1)	93.7(1)
							79.5(1)	100.0(1)	101.2(1)
							144.1(1)		
							153.4(1)		

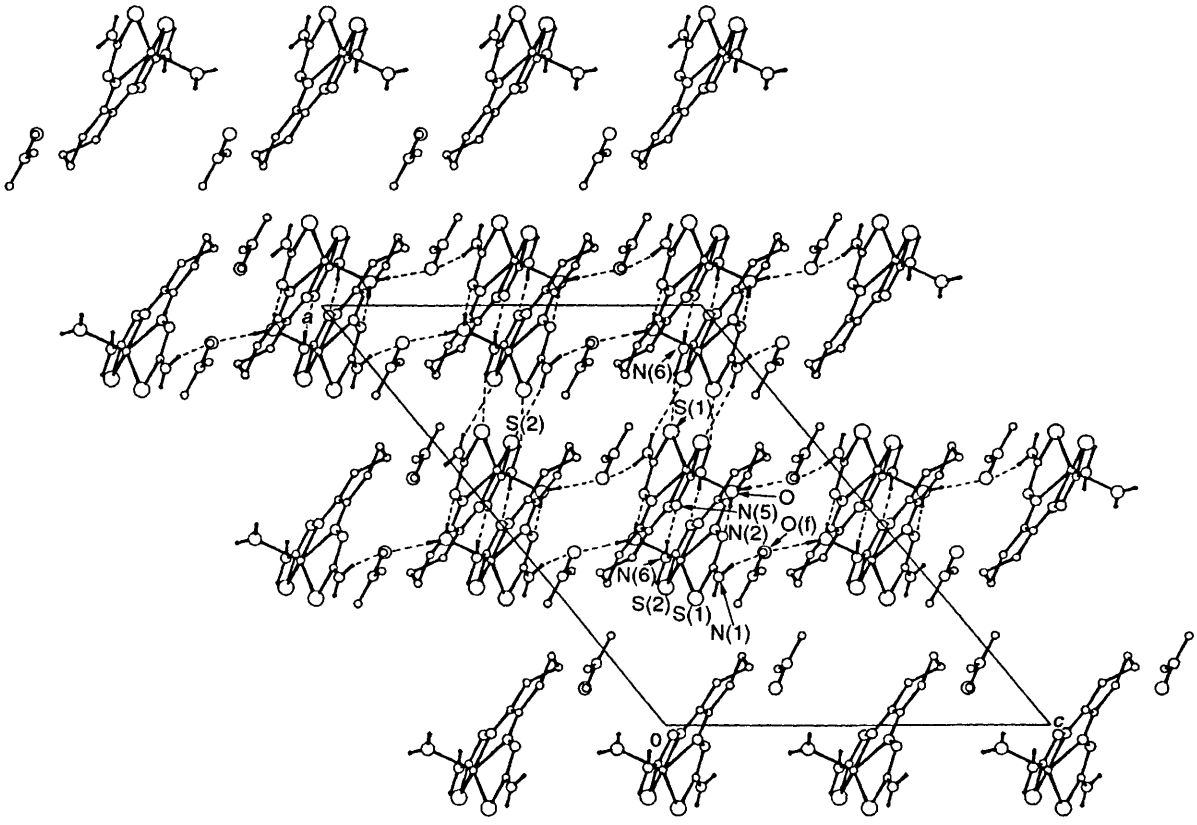

Fig. 3 The packing arrangement of complex **1**

Table 5 Bond distances (Å) in the ligand molecules for $[ZnL(OH_2)]\cdot dmf$ **1**, $[Zn(H_2L)Cl]Cl\cdot 2H_2O$ **2** and $[ZnL'(OH_2)]$ **3**[13]

Complex	S(1)–C(1)	S(2)–C(8)	C(1)–N(1)	C(8)–N(6)	C(1)–N(2)	C(8)–N(5)
1	1.737(5)	1.738(5)	1.339(8)	1.350(8)	1.316(6)	1.315(6)
2	1.637(7)	1.694(7)	1.314(9)	1.295(10)	1.345(9)	1.315(9)
3	1.735(4)	1.733(5)	1.346(5)	1.352(5)	1.325(5)	1.327(6)

Complex	N(2)–N(3)	N(4)–N(5)	C(2)–N(3)	C(7)–N(4)	C(2)–C(7)
1	1.384(6)	1.373(6)	1.283(6)	1.289(6)	1.499(8)
2	1.343(8)	1.319(8)	1.275(9)	1.255(9)	1.453(9)
3	1.374(4)	1.365(4)	1.281(6)	1.262(6)	1.470(5)

Table 6 Comparison of relevant torsion angles (°) in the ligands for **1**, **2** and **3**[13]

	1	**2**	**3**
S(1)–C(1)–N(2)–N(3)	2.4(8)	1.6(9)	6.5(5)
C(1)–N(2)–N(3)–C(2)	−170.4(6)	167.8(7)	−158.4(4)
N(3)–C(2)–C(7)–N(4)	5.5(8)	0.0(9)	−5.9(6)
C(7)–N(4)–N(5)–C(8)	168.8(6)	−173.0(6)	172.8(4)
N(4)–N(5)–C(8)–S(2)	−0.1(9)	1.3(9)	0.8(5)

chelate rings fall in the range 17.2–27.3 and 19.7–29.8° for **1** and **2** respectively.

The cyclohexane ring shows a nearly envelope and half-chair conformation in **1** and **2** respectively[15,16] [puckering parameters: $q_2 = 0.420(11)$, $q_3 = -0.254(10)$, $\varphi_2 = -12(1)$, $Q = 0.491(12)$, $\theta_2 = 121(1)$ in **1** and $q_2 = 0.367(8)$ Å, $q_3 = -0.317(8)$Å, $\varphi_2 = -18(1)°$, $Q = 0.485(8)$Å, $\theta_2 = 130.8(9)°$ in **2**]

In both complexes the packing interactions are very important (Table 7). In **1** the hydrogen bonds involving the hydrazinic nitrogen and oxygen atoms of centrosymmetrical molecules form dimer-like groups which are joined together through N–H · · · S bonds to form layers parallel to the (2 0 $\bar{2}$)

Table 7 Hydrogen bond distances (Å) and angles (°) in complexes **1** and **2***

D–H · · · A	D · · · A	D–H · · · A
Complex **1**		
N(1)–H(1) · · · O(f^{i})	2.92(1)	161(8)
N(1)–H(2) · · · S(2^{ii})	3.46(1)	158(8)
O(1)–H(13) · · · N(2^{iii})	2.79(1)	175(8)
N(6)–H(11) · · · N(5^{iv})	3.07(1)	168(7)
N(6)–H(12) · · · S(1^{v})	3.51(1)	163(5)
O(1)–H(14) · · · O(f^{vi})	2.89(2)	177(8)
Complex **2**		
N(2)–H(2) · · · Cl(2)	2.98(1)	156.4(3)
N(5)–H(5) · · · O(1)	2.73(1)	163.0(4)
N(6)–H(1N6) · · · O(1)	3.05(1)	137.6(4)
N(1)–H(1N1) · · · Cl(1^{vii})	3.31(1)	152.8(3)
O(2)–H(1O2) · · · Cl(2^{vii})	3.34(1)	166.7(5)
N(1)–H(2N1) · · · S(2^{viii})	3.50(1)	129.9(4)
O(1)–H(1O1) · · · O(2^{iii})	2.81(1)	149.6(4)
N(6)–H(2N6) · · · Cl(1^{iii})	3.30(1)	155.8(4)
O(2)–H(2O2) · · · Cl(1^{ix})	3.23(1)	127.6(7)

* Symmetry operations: i $x - \frac{1}{2}, y + \frac{1}{2}, z$; ii $\frac{1}{2} - x, y + \frac{1}{2}, \frac{1}{2} - z$; iii $1 - x, 1 - y, 1 - z$; iv $1 - x, -y, 1 - z$; v $\frac{1}{2} - x, y - \frac{1}{2}, \frac{1}{2} - z$; vi $x - \frac{1}{2}, \frac{1}{2} - y, z - \frac{1}{2}$; vii $\frac{3}{2} - x, y - \frac{1}{2}, \frac{3}{2} - z$; viii $x + \frac{1}{2}, \frac{1}{2} - y, \frac{1}{2} + z$; ix $x - \frac{1}{2}, \frac{1}{2} - y, z - \frac{1}{2}$.

Table 8 Selected vibrational bands (cm^{-1}) of H_2L and its metal complexes

	ν(OH), ν(NH_2)	ν(NH)	ν(CH)	ν(CN)	ν(CH), δ(NH_2)	δ(NCS)	ν(CS)	δ(CH), ν(CS)
H_2L	3402ms 3178ms	3111ms	2937m 2873w	1598s	1578m (sh) 1505s 1478vs	1075s	910ms	888m 837s
$Fe(H_2L)Cl_2$·0.5EtOH	3377mw 3245mw	3133m	2968mw 2871mw	1611vs	1539s 1453mw 1406m	1040w	923w	881w 813w
$Ni(H_2L)Cl_2$	3437m 3291m	3131m	2938mw 2860mw	1634vs 1613 (sh)	1577 (sh) 1471s 1418ms	1121s	927w	885mw 812w
$Cu(H_2L)Cl_2$	3400m 3177m	3112mw	2934w	1600s	1503 (sh) 1476vs	1076m	910m	885mw 834m
$Zn(H_2L)Cl_2$·EtOH	3371m 3318m 3243m	3129ms	2948w 2865mw	1613s	1542vs 1407ms	1111mw 1042mw	921w	881mw 795m
$[Zn(H_2L)Cl]Cl·2H_2O$	3566w 3374 (sh) 3307ms 3187 (sh)	3145 (sh)	2951w 2870w	1652 (sh) 1614vs	1559s 1430m 1408m	1117mw 1004mw	920mw	882m 816m (sh) 796ms
NiL	3475m 3282mw 3098mw	—	2926w 2855w	1630s	1581w 1536w 1492m 1452vs	1083w 1053w	971mw 931mw	890mw 822w
CuL·0.5EtOH	3472mw 3393ms 3280m 3171m	—	2927w	1623m	1594m 1534mw 1476s 1439vs	1082w	926mw	885mw 819w
ZnL·EtOH	3480 (sh) 3449m 3334ms 3274m 3127mw	—	2942mw	1622 (sh)	1597s 1531mw 1463m 1407vs	1044m	917mw	876mw 820mw
$[ZnL(OH_2)]$·dmf	3372m 3310ms 3194m 3130m	—	2943mw	1629m 1606ms	1536mw 1462ms 1422vs	1101w	975w 916mw	882mw 818w

Table 9 The ^1H NMR spectra (δ in ppm) of H_2L and its zinc complexes[a]

	N(5)H, N(2)H	$N(1)H_2$, $N(6)H_2$	$C(3)H_2$, $C(6)H_2$	$C(4)H_2$, $C(5)H_2$	EtOH	dmf
H_2L	12.21–7.28		2.52[b]	1.66 (br s)	—	- -
$Zn(H_2L)Cl_2$·EtOH	12.21–7.20		2.53[b]	1.66 (t)	1.04 (t) 3.43 (q) 5.15 (t)	- -
$[Zn(H_2L)Cl]Cl·2H_2O$	12.21–7.20		2.53[b]	1.66 (t)	—	- -
ZnL·EtOH	—	6.95s (4 H)	2.56[c] (4 H)	1.64[c] (4 H)	1.04 (t) 3.43 (q) 4.35 (t)	- -
$[ZnL(OH_2)]$·dmf	—	6.94s (4 H)	2.56[c] (4 H)	1.64[c] (4 H)	—	2.72 (s) 2.88 (s) 7.94 (s)

[a] For the numbering scheme see Figs. 1 and 2. [b] Partially obscured by the solvent signal. [c] Unresolved multiplet.

planes. The layers are interlinked by other hydrogen bonds [O–H · · · O(f) and N–H · · · O(f), O(f) = dmf oxygen] involving the dimethylformamide molecules (Fig. 3). In complex **2** the hydrogen interactions between the co-ordinated chlorine atom, Cl(1) and the amine nitrogens form chains running along the crystallographic *b* axis. The chains are hydrogen bonded to the chloride anions, Cl(2) [N(2)–H · · · Cl(2) 2.984(6) Å] and to the lattice water molecules (Fig. 4).

Infrared Spectra.—Selected vibrational bands of H_2L and its metal complexes are reported in Table 8. Some spectroscopic similarities are evident in each series of complexes derived from metal chlorides and acetates and containing the ligand in its neutral and deprotonated form respectively.

The solvated nature of the majority of the complexes and the presence of NH and NH_2 groups in the ligand molecule are responsible for the numerous vibrational absorptions in the 4000–3000 cm^{-1} region; the multiplicity of these bands, influenced by intra- and inter-molecular hydrogen bonds, makes a certain assignment of the ν(OH), ν(NH) and ν(NH_2) bands and the unequivocal disappearance of the ν(NH) bands in the ML complexes difficult to determine.

In the 1700–1500 cm^{-1} region, the ν(CO) due to the dmf molecule is clearly seen in the spectrum of the zinc complex (1669 cm^{-1}).

The shifts observed for the C=N groups suggest the participation of the imine group in the co-ordination to the metal atom. The assignment of the bands involving the C=S group is often uncertain, nevertheless the band at *ca.* 910 cm^{-1} in the spectrum of H_2L may be attributed to the C=S stretching mode even if this stretching mode probably also contributes to the bands observed at *ca.* 1100 and 880 cm^{-1}.[3,17,18]

The co-ordination of the sulfur atom to the metal is

Table 10 The ^{13}C NMR spectra (δ in ppm) of H_2L and its zinc complexes *

	C(1), C(8)	C(2), C(7)	C(3), C(4)	C(5), C(6)	EtOH	dmf
H_2L	179.28	146.30	27.31	21.20	—	—
$Zn(H_2L)Cl_2$·EtOH	179.44	146.46	27.49	21.76	56.38 18.94	—
$[Zn(H_2L)Cl]Cl·2H_2O$	179.43	146.44	27.47	21.36	—	—
ZnL·EtOH	178.53	143.87	26.69	21.46	56.23 18.77	—
$[ZnL(OH_2)]$·dmf	178.78	144.12	26.95	21.72	—	162.67 36.15 31.13

* For the numbering scheme see Figs. 1 and 2.

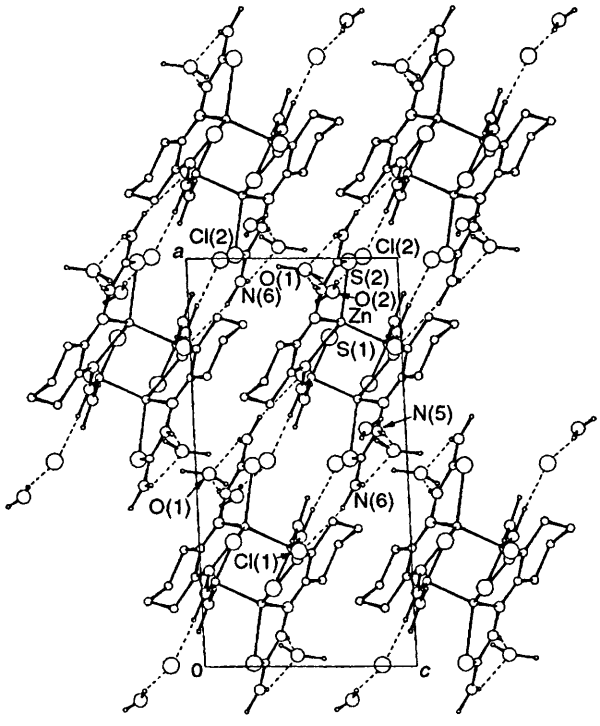

Fig. 4 Projection of the structure of complex **2** in the (010) plane

consistent with the shift (5–20 cm^{-1}) observed in the spectra of the metal complexes.

NMR Spectra.—The ^1H and ^{13}C NMR data of H_2L and its zinc complexes are reported in Tables 9 and 10. The ^1H spectrum of H_2L is very complex, owing to a large number of signals between δ 12.21 and 7.28 (all of them are influenced by the addition of some drops of D_2O, indicating the tendency to deprotonation), which could be due to the existence in solution of different tautomeric forms: nevertheless both the thiosemicarbazonic chains could be present in different conformations, as previously observed in cyclohexane-1,2-dione.[19] The two peaks at high field are assigned to the ring protons (Table 9). A similar complexity is observed in the ^{13}C spectrum of H_2L, where many peaks are again present, the most intense of which are listed in Table 10 and assigned according to previously reported data.[19,20]

The ^1H and ^{13}C spectra of the chloro complexes show a similar pattern to that observed for H_2L. The number and the position of the signals at high frequencies agree with the neutral nature of the ligand and indicate that several forms are present in solution in agreement with the results obtained from X-ray diffraction analyses (see above).

The spectra of the complexes containing the ligand in its deprotonated form are less complicated. In the ^1H spectrum (Table 9) all the down-field ligand peaks disappear consistent with the deprotonation of the N(5)H and N(2)H groups. The $N(1)H_2$ and $N(6)H_2$ groups show a single broad signal, indicating easier rotation about the C(1)–N(1) bond, probably due to a partial loss of multiplicity, as suggested by the changes in the bond distances[21,22] resulting from the involvement of the thiol group in co-ordination. The ring protons are slightly affected and the signals due to the dmf and EtOH molecules are clearly identified.

In the ^{13}C spectra (Table 10) the C(1) and C(8) atoms are shielded with respect to those in H_2L, indicating that the thione–thiol tautomerism[23] has a greater influence than the metal inductive effect and the π-delocalization in the molecule. The rearrangement of the electronic π charge probably causes the shielding observed in the C(2) and C(7) signals and the charge delocalization may also explain the slight shielding observed for the C(3) and C(4) atoms. The signals due to the solvent molecules are also clearly observed.

Acknowledgements

The authors thank the Ministero dell'Università e della Ricerca Scientifica e Tecnologica (MURST), Italy for financial support. M. C. R. A. is grateful for a grant from the Xunta de Galicia (Spain).

References

1 M. Belicchi Ferrari, G. Gasparri Fava, P. Tarasconi, R. Albertini, S. Pinelli and R. Starcich, *J. Inorg. Biochem.*, 1994, **53**, 13.
2 M. Belicchi Ferrari, G. Gasparri Fava, P. Tarasconi and C. Pelizzi, *J. Chem. Soc., Dalton Trans.*, 1989, 361.
3 M. Belicchi Ferrari, G. Gasparri Fava, C. Pelizzi and P. Tarasconi, *J. Chem. Soc., Dalton Trans.*, 1992, 2153.
4 M. C. Rodríguez-Argüelles, M. Belicchi Ferrari, G. Gasparri Fava, C. Pelizzi, P. Tarasconi, R. Albertini, P. P. Dall'Aglio, P. Lunghi and S. Pinelli, *J. Inorg. Biochem.*, in the press.
5 F. Ugozzoli, ABSORB, a program for Walker and Stuart's absorption correction, *Comput. Chem.*, 1987, **11**, 109.
6 G. M. Sheldrick, SHELXS 86, *Crystallographic Computing 3*, Oxford University Press, 1985.
7 A. Altomare, G. Cascarano, C. Giacovazzo, A. Guagliardi, M. C. Burla, G. Polidori and M. Camalli, SIR92, a program for automatic solution of crystal structures by direct methods, *J. Appl. Crystallogr.*, 1994, **27**, 435.
8 G. M. Sheldrick, SHELX 76, a program for crystal structure determination, University of Cambridge, 1976.
9 *International Tables for X-Ray Crystallography*, Kynoch Press, Birmingham, 1974, vol. 4.
10 M. Nardelli, *Comput. Chem.*, 1983, **7**, 95.
11 C. K. Johnson, ORTEP, Report ORNL-3794, Oak Ridge, TN, 1965.
12 W. D. S. Motherwell, PLUTO, University of Cambridge, 1976.
13 P. E. Bourne and M. R. Taylor, *Acta Crystallogr., Sect. B*, 1980, **36**, 2143.
14 L. Pauling, *The Nature of the Chemical Bond*, Cornell University Press, Ithaca, NY, 1960.

15 D. Cremer and J. A. Pople, *J. Am. Chem. Soc.*, 1975, **97**, 1354.
16 J. C. A. Boeyens, *J. Cryst. Mol. Struct.*, 1978, **8**, 317.
17 M. J. M. Campbell, *Coord. Chem. Rev.*, 1975, **15**, 279.
18 S. Padhye and G. B. Kauffman, *Coord. Chem. Rev.*, 1985, **63**, 127.
19 D. V. Rao, F. A. Stuber and H. Ulrich, *J. Org. Chem.*, 1979, **44**, 456.
20 A. Macías, M. C. Rodríguez-Argüelles, M. I. Suárez, A. Sánchez, J. S. Casas and J. Sordo, *J. Chem. Soc., Dalton Trans.*, 1989, 1787.
21 J. S. Casas, M. V. Castaño, M. C. Rodríguez-Argüelles, A. Sánchez and J. Sordo, *J. Chem. Soc., Dalton Trans.*, 1993, 1253.
22 J. S. Casas, M. V. Castaño, M. S. García-Tasende, I. Martínez-Santamarta, A. Sánchez, J. Sordo, E. E. Castellano and J. Zukerman-Schpector, *J. Chem. Res.*, 1992, (*S*) 324.
23 A. M. Brodie, H. D. Holden, J. Lewis and M. J. Taylor, *J. Chem. Soc., Dalton Trans.*, 1986, 633.

Received 24*th January* 1995; *Paper* 5/00396B